Cold acclimation and deacclimation in wild blueberry: Direct and indirect influence of environmental factors and non-structural carbohydrates

Annie Deslauriers, Léa Garcia, Guillaume Charrier, Valentinà Buttò, André Pichette, Maxime Paré

Cold acclimation and deacclimation in wild blueberry: direct and indirect influence of environmental factors and non-structural carbohydrates

Annie Deslauriers[1], Léa Garcia[1], Guillaume Charrier[2], Valentinà Buttò[1], André Pichette[1], Maxime Paré[1]

[1] Centre de recherche sur la Boréalie (CREB), Département des Sciences Fondamentales, Université du Québec à Chicoutimi, 555 boulevard de l'Université, Chicoutimi (Québec), Canada, G7H 2B1.

[2] Université Clermont Auvergne, INRAE, PIAF, F-63000 Clermont-Ferrand, France.

Abstract

Through the annual cycle of plant growth and dormancy, the winter season leads to profound metabolic changes allowing plants to undergo cold acclimation. In boreal environments, winter conditions are changing rapidly and are likely to cause damage to commercial wild lowbush blueberry. In this study, we addressed the level of frost hardiness and determined the role of environmental factors and non structural carbohydrates (NSCs) on frost hardiness. From autumn to spring, stem sections of *Vaccinium angustifolium* and *Vaccinium myrtilloides* were harvested each month in a commercial blueberry field to assess the relative electrolyte leakage and calculate the temperature at which 50% of the cells are lysed [LT_{50} (°C)], used as frost hardiness index. Stems were also collected to assess soluble carbohydrates and starch. Correlations, principal component analysis (PCA) and structural equation modelling (SEM) were used to determine how environmental factors and NSCs directly or indirectly influence the frost hardiness index. Frost hardiness reached its lowest level in December and January with LT_{50} dropping below -60 °C. Seasonality of frost hardening was closely linked to photoperiod and temperature, generating clock-wise hysteretic loops that divide frost hardening into acclimation, from September to January, and deacclimation, from January to the end of May. Environmental factors such as photoperiod and temperature were more important in determining the level of frost hardiness during acclimation, with either direct or indirect effect through an influence on starch degradation, increasing soluble carbohydrate content. During deacclimation, soluble carbohydrates, especially raffinose, further induced a stronger direct regulation of frost hardiness. Direct biological regulation through raffinose defined the level of frost hardiness during deacclimation. However, the negative influence of temperature on raffinose concentration could increase vulnerability to winter warming events.

Keywords: *Vaccinium angustifolium*, cold hardiness, temperature, photoperiod, snow depth, raffinose

1. Introduction

In boreal habitats, daily temperatures exhibit a very wide annual range: from about -40 to +30 °C. To survive harsh winter conditions, boreal shrubs inhibit their growth potential through the process of dormancy and acclimation to cold (Arora and Rowland, 2011; Charrier et al., 2011; Strimbeck et al., 2015). This process occurs in response to climate stimuli (Maurya et al., 2018; Strimbeck et al., 2008), and can thus be affected by global warming. Under climate change, winter conditions are expected to fluctuate, with higher temperature variability and increasing occurrence of polar vortices (Anderson and Gough, 2017; Yu and Zhang, 2015). Decreasing snow cover depth through a change in the balance between solid (snow) and liquid precipitations would induce more frequent freeze-thaw cycles (Williams et al., 2015). Boreal shrubs overwintering beneath the snow, such as lowbush blueberry (*Vaccinium angustifolium* Aiton and *Vaccinium myrtilloides* Michx), are extremely sensitive to snow cover. Indeed, a snow depth threshold of 30 cm has been identified in commercial fields in order to protect lowbush blueberry stems and buds throughout winter (Girona et al., 2019; Wildung and Sargent, 1989). In northern environments, winter damage is considered a major factor limiting blueberry fruit yields (MAPAQ, 2016; Moore, 1994). Indeed, winter warming predisposes overwintering boreal and arctic shrubs such as *Vaccinium* spp. to spring-like physiological development, possibly reducing subsequent growth, flowering, berry production or causing plant death (Bokhorst et al., 2010). Under such challenging conditions, there is a growing need to study the adaptation of plant species throughout the frost-exposed period, from autumn to spring (Arora and Taulavuori, 2016; Die et al., 2016; Palacio et al., 2015; Rowland et al., 2008). Better understanding cold acclimation and deacclimation of wild blueberry species would also help producers to better predict subsequent fruit yields when temperatures are extremely cold during autumn-spring periods.

45 In temperate and boreal environments, aboveground parts exhibit cold acclimation from autumn to winter,
46 which transiently increases their freezing tolerance, and deacclimation from winter to spring (Charrier et
47 al., 2013). In woody plants, cold acclimation is first initiated by decreasing photoperiod during late
48 summer, under non-freezing temperature, and then by cold and freezing temperature in a second stage (Li
49 et al., 2004). Compared to trees, boreal shrubs overwinter beneath the snow and thus avoid very low
50 atmospheric temperatures. Indeed, although the environment beneath the snow is more stable, i.e.
51 attenuation of temperature variations (Saarinen and Lundell, 2010), we have little information on the effect
52 of temperature and snow cover on the frost hardiness of wild lowbush blueberry.

53 During cold acclimation, carbohydrates content increases as the starch reserves decrease, with opposite
54 patterns during the period of deacclimation (Baffoin et al., 2020; Charrier et al., 2018a; Charrier et al.,
55 2013). By increasing carbohydrate content during autumn, starch conversion indirectly contributes to
56 freezing tolerance, as shown in *Trifolium pratense* L. (Bertrand et al., 2020). For many plant species,
57 raffinose is an important carbohydrate for cold resistance during winter (Kasuga et al., 2007; Sauter,
58 1988). Raffinose acts as cellular cryoprotectant allowing the stabilization of cell membranes through
59 hydrogen bonds with membrane phospholipids, thus protecting the cell structures from frost-induced
60 dehydration (Xin and Browse, 2000). In addition, accumulation of soluble carbohydrates in living tissues
61 of stem and buds leads to a decrease in the freezing point, enhancing the probability of extracellular ice
62 formation (Lee et al., 2012; Sauter, 1988). In addition to being mobile and translocated in phloem, sucrose
63 also has a protective effect that is not based solely on osmosis effect, but also has a cryoprotective activity,
64 stabilizing membranes and proteins (Imanishi et al., 1998), while glucose is important in providing energy
65 for metabolism during the winter (Beauvieux et al., 2018; Die et al., 2016). The increase in solutes thus
66 exerts a protective effect through an increase in the solute content, decreasing the freezing temperature
67 and limiting the dehydration generated by ice formation (Baffoin et al., 2020; Charrier et al., 2013). It is

68 therefore important to understand the dynamics of the conversion between soluble carbohydrates and
69 starch through frost acclimation and deacclimation in order to predict the frost vulnerability of *Vaccinium*
70 spp.

71 Environmental factors such as temperature and photoperiod, can act both directly or indirectly by
72 activating important metabolic processes (Die and Rowland, 2014; Ibáñez et al., 2010). Other
73 environmental factors, such as snow cover, act by providing an insulating effect from extremely cold
74 temperature (Ambroise et al., 2020; Girona et al., 2019; Palacio et al., 2015; Wildung and Sargent, 1989).
75 In taller plants such as walnut trees, both photothermal and thermal models were able to correctly predict
76 frost hardiness (Charrier et al., 2018a), indicating the importance of temperature and photoperiod in
77 controlling the process involved. Even though temperature and photoperiod are correlated at higher
78 latitudes, no additive effect (i.e. partial composition of frost hardiness under distinct temperature and
79 photoperiod effects) was found on frost hardiness for Scots pine (Zhang et al., 2003), indicating specific
80 and distinct roles for each of these two environmental factors.

81 In commercial wild lowbush blueberries, frost resistance studies have mainly been restricted to hybrids of
82 *Vaccinium corymbosum* (Lee et al., 2013; Rowland et al., 2008), and the European species *Vaccinium*
83 *myrtillus* L. (Palacio et al., 2015; Taulavuori et al., 1997). Although endemic blueberry shrubs of North
84 America, including *Vaccinium angustifolium* Aiton and *Vaccinium myrtilloides* Michx, represent an
85 important export for the Canadian economy [more than 200 million $\$\cdot year^{-1}$ (MAPAQ, 2016)], they have
86 rarely been investigated with respect to cold acclimation and deacclimatation (Cappiello and Dunham,
87 1994). The study of non-structural soluble carbohydrates (NSCs), along with the key environmental
88 parameters (photoperiod, temperature and snow depth), could therefore provide valuable information on
89 the changes that occur in cold acclimation and deacclimation in wild blueberries. The main objectives of
90 this study were to (1) assess the level of frost hardiness, measured as LT_{50} (i.e. the lethal temperature at

which 50% of cells are lysed), in wild blueberry from autumn to spring and (2) determine the correlation between environmental factors, NSCs and frost hardiness. We tested the hypothesis that environmental factors directly influence the building NSCs for cryoprotection in the stem and that both environmental factors and NSCs are linked with the frost hardiness index (Figure 1).

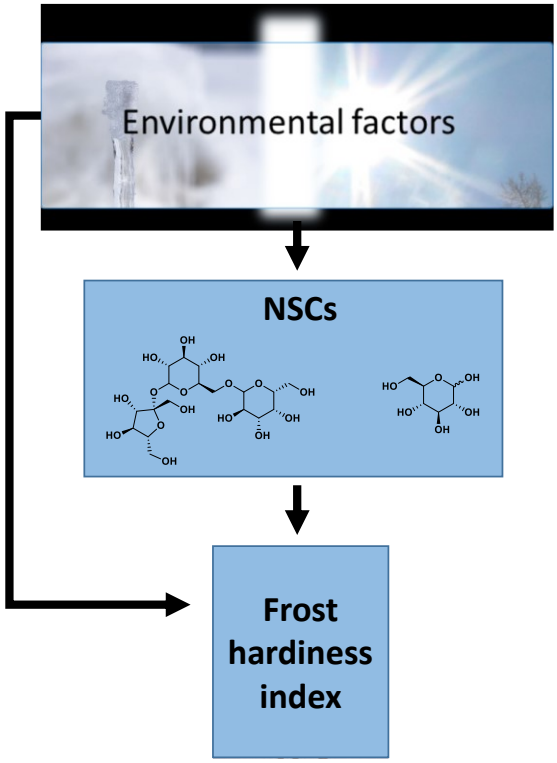

Figure 1. Assumptions behind the conceptualization of the structural equation models (SEM) linking environmental variables, NSCs and frost hardiness index. In the middle, the structure of raffinose (left) and glucose (right) represent examples of NSCs.

2. Material and methods

This study was conducted in a commercial wild lowbush blueberry field at the "Les Entreprises Gérard Doucet Ltée" in Saint-Honoré, Saguenay-Lac-Saint-Jean, Quebec, Canada (48°31′16″N; 71°00′35″W, 160m a.s.l.). More than 80% of the Quebec wild blueberry fields are located in the

Saguenay-Lac-Saint-Jean area (MAPAQ, 2016; Vander Kloet, 1988). In this region, the climate is humid continental with a moderately warm summer (Figure 2). Average daily temperatures range from -17 °C in winter to 18 °C in summer (Figure 2) and minimum and maximum temperatures from -29 °C to 27 °C (Figure 2). Because of high snow accumulation during winter [mean maximum snow cover of 77 cm from 1980 to 2019, Environment Canada (2019)], a systematic sampling design along 6 transect lines was implemented to avoid digging beneath the snow near a previous sampling point. The use of transect lines allow indeed to perform a systematic sampling, where samples are collected at fixed intervals of 5 meters along each line, but at different dates (Bonham, 2013). Two transect lines per field were established in three blueberry fields separated by mature Jack pine trees (*Pinus banksiana*, Lambs). The lines were on each side of the field, at 13 meters from the border trees. Every month, stems of blueberry were randomly collected (see next section) along the transect line at 5 meter intervals. During winter, a space of about 1 × 2 meters was dug in the snow to reach the plants (supplementary material, Figure S1). During sampling, from September 2018 to June 2019, blueberry plants had both vegetative and floral buds.

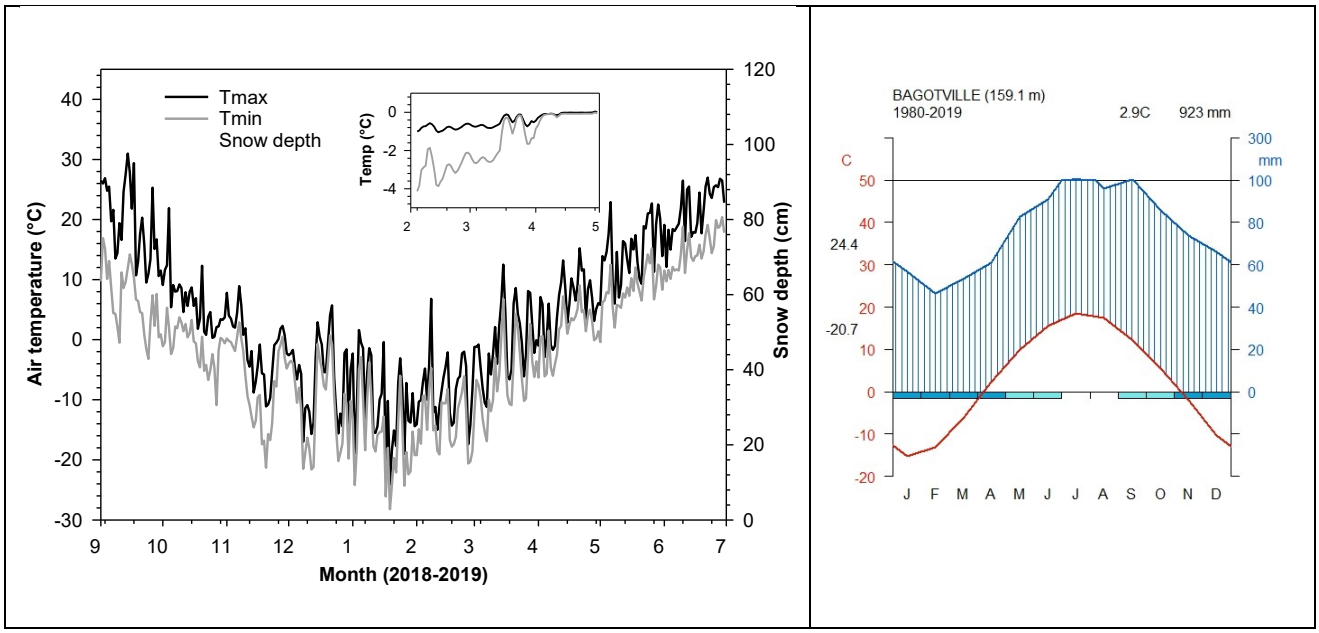

Figure 2. Left part: Maximum (black line) and minimum (gray line) air temperature (°C) and snow depth (gray background, cm) recorded at the Bagotville station from September 2018 to July 2019.

Inset: Mean temperature (°C) at the soil-snow interface, at two sampling points from February to May 2020. Right part: Walter & Lieth climatic diagrams representing average climatic conditions [mean temperature (red line), mean precipitation (in blue)] at the nearest weather station (Bagotville). The blue rectangles represent months with below zero temperature while the cyan rectangles indicate months when below zero temperatures are highly probable.

Two species of wild blueberry were sampled, *Vaccinium angustifolium* Aiton and *Vaccinium myrtilloides* Michx, because species distinction was not possible beneath the snow during winter (supplementary material, Figure S1). These species also form hybrids, even having distinct genetics and phenology (Fournier et al., 2020). Both are grown together as mixed vegetation in commercial fields in the north of Quebec (Canada). At each sampling date, 24 stems were cut at the base of the plant to measure the non-structural soluble carbohydrates (NSC) concentration (4 stems × 6 transects) and 96 were cut to measure frost hardiness (16 stems × 6 transects). During sampling, performed in the morning, the plants were placed in a test tube, wrapped in wet absorbent paper around the base to prevent dehydration and kept in a cooler. In the laboratory, the stems used for NSC measurement were stored in a freezer at -17 °C for 1-2 days until liquid nitrogen immersion, while those collected for frost hardiness were treated immediately.

2.1 Frost hardiness

At each sampling date from September 2018 to June 2019, two whole stems from each transect were wrapped in moist paper and aluminum foil and exposed to controlled temperature treatments. To measure the temperature during the frost treatment, a thermocouple probe, connected to a data logger (CR100, Campbell Scientific) was placed in the middle of the blueberry stems. The stems and probes were then inserted in 7 insulated thermos and placed in a cold room (Envirotronics EH40-2-3). The temperature inside the room gradually decreased from 5 °C to -50 °C at a rate of about $5K \cdot h^{-1}$. Seven target temperatures were selected: the first was set at 5 °C (control temperature assuming minimum damage to

140 the samples) while -1 °C, -10 °C, -20 °C, -30 °C, -40 °C and -50 °C represented progressive frost damage.
141 Maximum damage was assumed to occur in a seventh thermos exposed to -80 °C in an ultra-low
142 temperature freezer (Thermo Scientific, Forma 88000 Series).

143 Once the target temperature had been reached, the thermos were removed from the cold room and placed
144 at 5 °C overnight to ensure a slow thawing. Subsequently, the buds were all removed and several small
145 stem sections (of ~ 2-3 mm, excised between the buds) were cut with a surgical scalpel to increase
146 electrolyte release in the solution and thereby obtain more accurate lysis values. The stem sections were
147 then placed in a 30 ml vial filled with 10 ml of ultrapure water. A pressure of -50 bar was applied for 3
148 minutes and then the vials were placed on stirring plates for 20 hours with gentle agitation (Lee et al.
149 2012). Two conductivity measurements were then performed using a conductimeter (ThermoScientific
150 Orion Star A112), before (C_1) and after (C_2) autoclaving the vial for 30 minutes (121 °C, 17 PSI). Relative
151 electrolyte leakage (REL) was calculated according to the following formula:

152 $$\mathrm{REL} = \frac{C_1}{C_2} \qquad (1)$$

153 where C_1 is the conductivity of the electrolyte solution measured after the cold treatment and C_2 is the
154 conductivity of the electrolyte solution measured after autoclaving.

155 The relationship between REL and temperature was then calculated according to the following four
156 parameter sigmoidal relationships by using either each of the six transects individually or by pooling the
157 data of all transects (Charrier et al., 2018a):

158 $$REL = \frac{a}{1+e^{b(c-\theta)}} + d \quad (2)$$

where θ is the temperature (°C) of the cold resistance test (including controls at 5 °C and -80 °C), the parameters *a* and *d* define the upper (maximum lysis) and lower (minimum lysis) asymptotes of the sigmoid function and *b* is the nonlinear slope at the point of inflection *c*.

Between the upper and lower asymptotes, the 50% relative electrolyte leakage corresponds to the point of inflection (c) of the sigmoid curve. This point of inflection, estimated directly by the parameter c, corresponds to the temperature at which 50% of cells are lysed or to the lethal temperature at 50%, LT_{50} (°C). This threshold (LT_{50}) was used as a dynamic frost hardiness index over the winter. Parameter estimation was performed by a non-linear regression procedure (PROC NLIN) using the SAS analysis software.

2.2 NSC extraction

At each sampling date, the stems sampled in each transect (4 per transect) were pooled to obtain sufficient material (> 50 mg DM) for NSC extraction (soluble carbohydrates and starch). The stems were immersed in liquid nitrogen and placed in a freeze-dryer for one week until complete desiccation. Once the samples were dry, they were ground using a ball mill (vibrating mill MM 200, Retsch).

For carbohydrates solubilisation, 10 mg of dry powder of stems was placed in a 15 ml test tube and mixed with 5 ml of 20% ethanol (HPLC grade) and 100 µl of 1% sorbitol representing an internal standard. The samples were centrifuged for 10 minutes, and the supernatants were kept apart. These steps were repeated three times, but the internal standard was added only during the first extraction. The supernatant mixture was evaporated to remove the alcohol and resolubilized in 2 ml of water. The samples were then passed through an ion exchange resin: CH and N + Quaternary amino, to separate the carbohydrates and polyols from the undesired compounds. The fraction of carbohydrates and polyols was evaporated, resolubilized in 2 ml of water and then finely filtered using a nylon syringe filter (0.45 µm pore size) and injected with HPLC-RID (Agilent 1200 series) on a Shodex SC 1011 column sugar series. The carbohydrate

concentrations were then determined using standard curves made for each of the identified carbohydrates: sucrose, glucose, fructose, raffinose and stachyose (Deslauriers et al., 2014).

The pellets recovered following carbohydrates analysis were used to measure the starch concentration (Bellasio et al., 2014). The enzymes α-amylase (Megazyme - 3000 U / L), allowed the starch chains to be split into oligosaccharides and dextrins. Shorter, unbranched chains were then hydrolyzed by a second enzyme, amyloglucosidase (Megazyme - 3260 U / L). The α-amylase-buffer solution (composed of 850 ml of distilled water, 5.8 ml of glacial acetic acid, 1M NaOH and 0.74 g of dehydrated $CaCl_2$) was mixed and incubated for 12 minutes at 90-100 °C. A volume of 0.15 ml of the second enzyme, amyloglucosidase, was then added and the samples were incubated for 45 minutes at 50 °C. The volume in the tubes was subsequently adjusted to 10 ml with distilled water and after being centrifuged for 6 minutes, the supernatant was recovered for subsequent analysis. Then 2 ml of Reagent solution (made from 100 ml of distilled water, 1 capsule of peroxidase (PGO) and 1.6 ml of ortho-dianisidine) was added to each of the tubes. Peroxidase (PGO) oxidized glucose to gluconic acid with quantitative production of hydrogen peroxide which in turn oxidized the dye (ortho-dianisidine). After standing for 45 minutes in the dark, 400 µL of 75% H_2SO_4 was added, as starch is hydrolyzed in acidic condition. The absorbance was then measured after 20 min at 530 nm using a UV-VIS spectrophotometer. Starch concentrations were then converted to mg per g dry weight ($mg \cdot g^{-1}dw$).

2.3 Statistical analysis

In order to test our hypothesis (Figure 1), two types of analysis were conducted, principal component analysis (PCA) and structural equation modelling (SEM). While PCA aims at representing the variation between sampling dates by using all measured variables (frost hardiness index, NSCs and environmental factors), SEM aims at exploring multiple pathways by which environmental factors and NSCs determine, directly and indirectly the modulation of the frost hardiness index (Grace, 2006). For both analysis, the

205 LT_{50} values used as a frost hardiness index, were linked to the environmental variables. Means were
206 performed by using different time windows varying from 1 to i days prior to the sampling date with i
207 ranging between 5 to 20 days. Mean temperature (°C), mean of daily maximum and minimum temperature
208 (°C), mean photoperiod and mean snow depth (cm) were computed from hourly data from the Bagotville
209 station (Environment Canada (2019). Linear correlations (Pearson, CORR procedure in SAS) were
210 performed between LT_{50} and the computed means to select the time window with the highest correlations.
211 Further cross-correlations were performed by moving the different time windows from 1 to j time lag with
212 j ranging between 1 to 55 days. The correlations between LT_{50} and environmental factors were highest by
213 using a window of 5 days before the sampling with no time lag (supplementary material, Figure S2).

214 Principal component analysis (PCA) was performed to study the relationship between all the variables.
215 Pearson's correlation coefficients between variables and axes, and contribution percentage (%) of each
216 variable for the main PCA's axes were extracted using the R package FactoMineR (Lê et al. 2008; R Core
217 Team 2019), while PCA was performed by means of R's package factoextra (Kassambara and Mundt
218 2020). Direct and indirect effects of the environmental factors and NSCs on LT_{50} were then tested by
219 means of multi-group structural equation models (SEM), fitted separating acclimation (September to
220 January) from deacclimation (January to May), based on the hysteresis pattern of LT_{50} with environmental
221 factors (see results for more detail).

222 Models structures (Figure 1) were based according to the hypothesis that LT_{50} depends on the interplay
223 of both endogenous (NSCs) and exogenous factors (environment), whose influence changes according to
224 the time of the year. Endogenous factors such as soluble carbohydrates and starch are quantitative
225 variables that can explain frost hardiness (Bertrand et al., 2020), whereas exogenous are rather empirically
226 correlated. The environmental factors were represented by photoperiod (hours), mean temperature (°C)
227 and snow depth (cm). Because soluble carbohydrates were highly co-related (see result of PCA), we

228 considered that LT_{50} was related to the amount of raffinose, because this carbohydrate is one of the most
229 correlated with the frost hardiness index (Lee et al., 2012; Sauter, 1988; Strimbeck et al., 2008). The
230 amount of raffinose also depends on the environmental factors and amount of starch found in the plant at
231 the same time (Lee et al., 2012). In raspberry, the increase in soluble carbohydrate was mostly explained
232 by starch hydrolysis (Palonen et al., 2000) justifying an indirect link, via starch, between environmental
233 factors and raffinose. In order to study the effect of each environmental factor on raffinose and on LT_{50},
234 we performed three different multigroup Structural Equation Models (SEM) using one environmental
235 variable at a time but leaving the other variables and relationships unchanged. Multicollinearity between
236 variables was avoided by the assessment of their variance inflation factors (VIFs), retaining only those
237 having a VIF value <10 (Zuur et al., 2010). Multigroup SEM analysis was performed by means of lavaan
238 Rs package (Rosseel, 2012), with 10000 bootstrap resamples and Bollen-Stine bootstrapped P value (P_{bs})
239 was used to test model significance as it is more adapted to small samples (Beaujean, 2014; Hooper et al.,
240 2008). Models were accepted when $P_{bs} > 0.05$. All SEM analyses were performed by means of lavaan Rs
241 package (Rosseel, 2012), with 10000 bootstrap resamples (Beaujean, 2014). The effect of environmental
242 factors on LT_{50} and on NSCs concentration was assessed by comparison of the R^2 and the standardized
243 coefficients (std) of their relationships in the different models.

244 # *3.* Results

245 ## *3.1 Relative electrolytes leakages and LT_{50}*

246 The pattern of Relative Electrolyte Leakage (REL) changed drastically from September to October,
247 remained similar until mid-May and then changed again (Figure 3, left panel). These fittings were
248 performed by pooling all transect sampling points for a given date. The relations between REL and
249 exposed temperature were all highly significant (P<0.001), except in December (P=0.036). Lower
250 asymptotes were relatively constant (0.21 ± 0.09), except on December 5th and May 14th. In December,

higher minimum REL were observed compared to the other dates (0.45± 0.04, Figure 3). The higher asymptotes remained relatively constant at 0.70 ± 0.08. However, from mid-May to June, the higher asymptote was much more variable, exhibiting higher (May 29) or lower values (May 14 and June 11) than 0.70. Important changes in the REL pattern mostly occurred between September and October and from April to May (Figure 3).

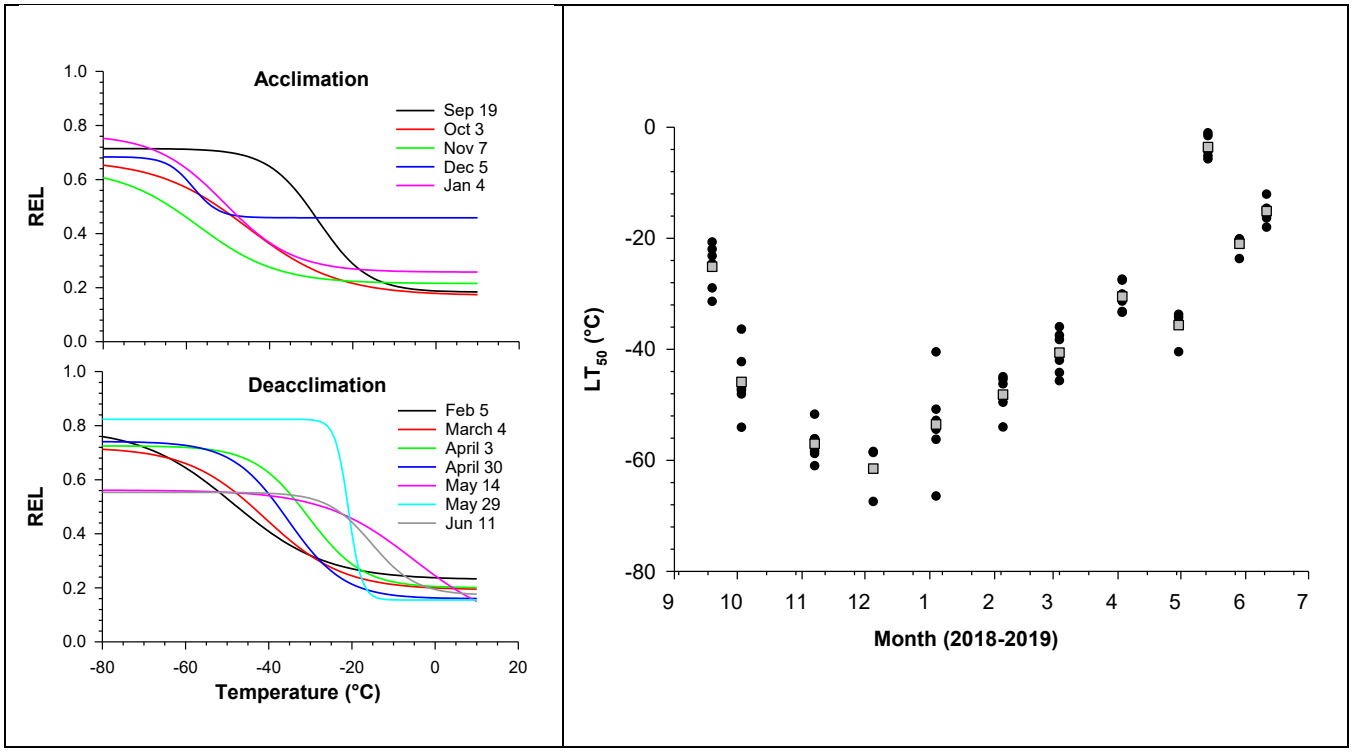

Figure 3. Left part: Relationships between electrolyte leakage (REL) and temperature (°C) calculated according to a sigmoidal relationship for the different sampling dates by using all transect sampling points. Curve fittings were performed by using all transect data points (black dots, illustrated in the graph on the left). Right part: LT_{50} (°C) of each transect line (black dots) and mean LT_{50} (gray square) for the different sampling dates.

LT_{50} in the different transects varied between -20 °C and -30 °C in September, gradually decreased in autumn to reach a minimum in December (Figure 3, right side). During the same period, the average air temperatures decreased from about 20 °C to -10 °C (Figure 2, left side). The minimum frost hardiness

individual values for a single plot were observed in December and January: LT_{50} dropped to -67 °C and -66 °C in December and January, respectively (Figure 3). With only 3 fitted sigmoid regressions out of 6, the coldest frost resistance temperature was calculated on December 5th, 2018, with LT_{50} varying between -58 °C and 67 °C. At that time, snow depth was about 20 cm and the absolute maximum and minimum air temperature recorded the week before the sampling was 0.8 °C and -14 °C, respectively (Figure 2). In January, LT_{50} values varied between -66 °C and -40 °C, while temperatures were still decreasing but snow depth increasing (Figure 2). From January until the beginning of April 2019, LT_{50} gradually increased. Afterwards, high LT_{50} variability was observed. During the sampling conducted on April 30th, 2019, frost hardiness dropped back to -35 °C while only traces of snow remained on the ground with air temperatures oscillating around - 5 °C (Figure 2). In mid-May, LT_{50} reached -5 °C when minimum air temperatures approached 10 °C (Figure 2).

3.2 Correlation and hysteresis between LT_{50}, NSC and environmental cues

Correlation between LT_{50} and environmental factors (mean temperature, photoperiod and snow cover), performed by using different time windows (from 5 to 20 days) and different time lags (from 0 to 55 days before the sampling) were higher by using a time window of 5 days and a time lag of 1 day (i.e. from 1 to 6 days prior to the sampling) (Supplementary Figure S2). Similar results were obtained for the correlation between NSC and environmental variables, except for that between starch and photoperiod which was slightly higher at a time lag of 15 days prior to sampling. For mean temperature and photoperiod, the correlation with LT_{50} or starch decreased with increasing time lag while the correlation increased with snow cover by increasing the time lag. For raffinose, the negative correlations increased with time lag for mean temperature and photoperiod while they decreased for snow cover. However, at lag 1, the correlation between raffinose and snow pack was very weak (Supplementary Figure S2).

286 Clockwise annual hysteresis patterns were observed between LT_{50} and temperatures (Figure 4). For
287 minimum, maximum and mean temperature, the decrease in LT_{50} followed the decrease in temperature
288 from September until December when the hysteresis loop is formed. Thereafter, LT_{50} values increased
289 with temperature, but with higher values compared to the previous decrease (Figure 4). The loop between
290 photoperiod and LT_{50} was similar to that of the temperatures but with a crossover value between
291 September and October because of the fast decrease in photoperiod at that time of the year. On the
292 contrary, a counter-clockwise loop was observed between snow depth and LT_{50} (Figure 4). However, the
293 loop with snow depth had a different form, with two direction changes between November and December
294 (i.e. when snow started to accumulate, Figure 2) and between March and April (i.e. when snow started to
295 melt, Figure 2). Except for starch, no hysteresis patterns were found between LT_{50} and sugars
296 concentrations, which rather presented a correlative pattern. For starch, hysteresis was detected with a
297 clockwise pattern.

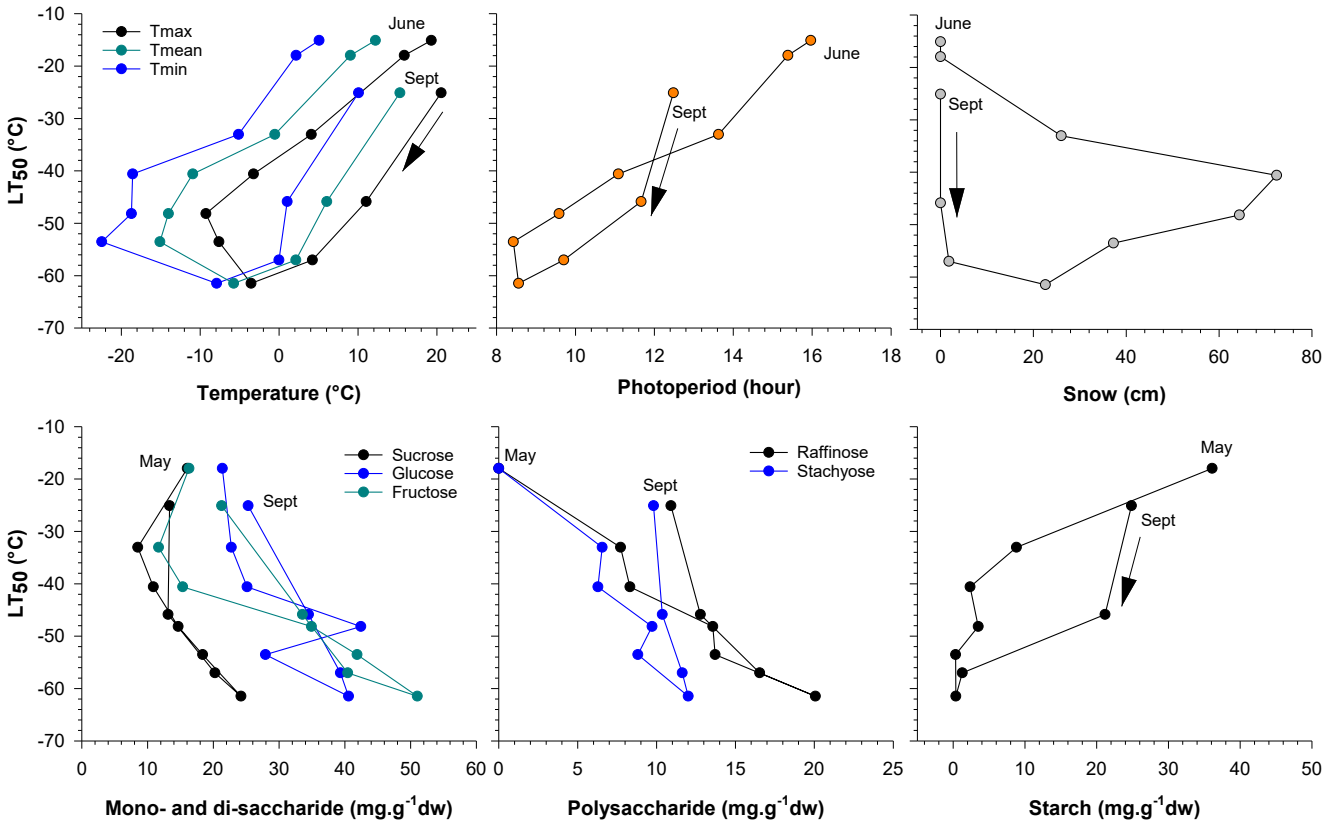

298 **Figure 4.** Higher part: Seasonal hysteresis between LT_{50} (°C) and meteorological variables [maximum,
299 mean, and minimum temperature (°C) averaged over 5 days, snow depth (cm), and photoperiod (hour)]
300 at monthly scale. Lower part: Relationship between LT_{50} (°C) and soluble sugars [sucrose, glucose,
301 fructose, stachyose and raffinose, expressed in $mg.g^{-1}dw$]. Seasonal hysteresis between LT_{50} (°C) and
302 starch concentration ($mg.g^{-1}dw$). The direction of the hysteresis, if present, is indicated with an arrow.

303 ***3.3 Carbohydrates concentration in the stem and link with LT_{50} and environmental factors***

304 In stems, glucose, fructose sucrose and raffinose concentrations showed, more or less, a bell-shaped curve
305 with an increase during autumn, a maximum in December, then a decrease during winter and spring
306 (Figure 5). The concentrations of glucose and fructose were thus higher from November to February with
307 concentrations close to or higher than 40 $mg.g^{-1}dw$. Both glucose and fructose had higher concentration

than sucrose, which reached a peak in December with about 25 mg.g^{-1}dw. The concentration of raffinose increased from September to February with slight variations between 10 and 20 mg.g^{-1}dw then it decreased from March and became null in May (Figure 5). Raffinose and stachyose concentrations were low compared to the other non-structural carbohydrates. The concentration of stachyose approached 10 mg.g^{-1}dw. Then, like raffinose, its concentration became null in mid-May. The starch concentration rapidly decreased from September to October with concentration almost null from November until January. The starch concentration then re-started to increase in February exhibiting an exponential increase during May (Figure 5).

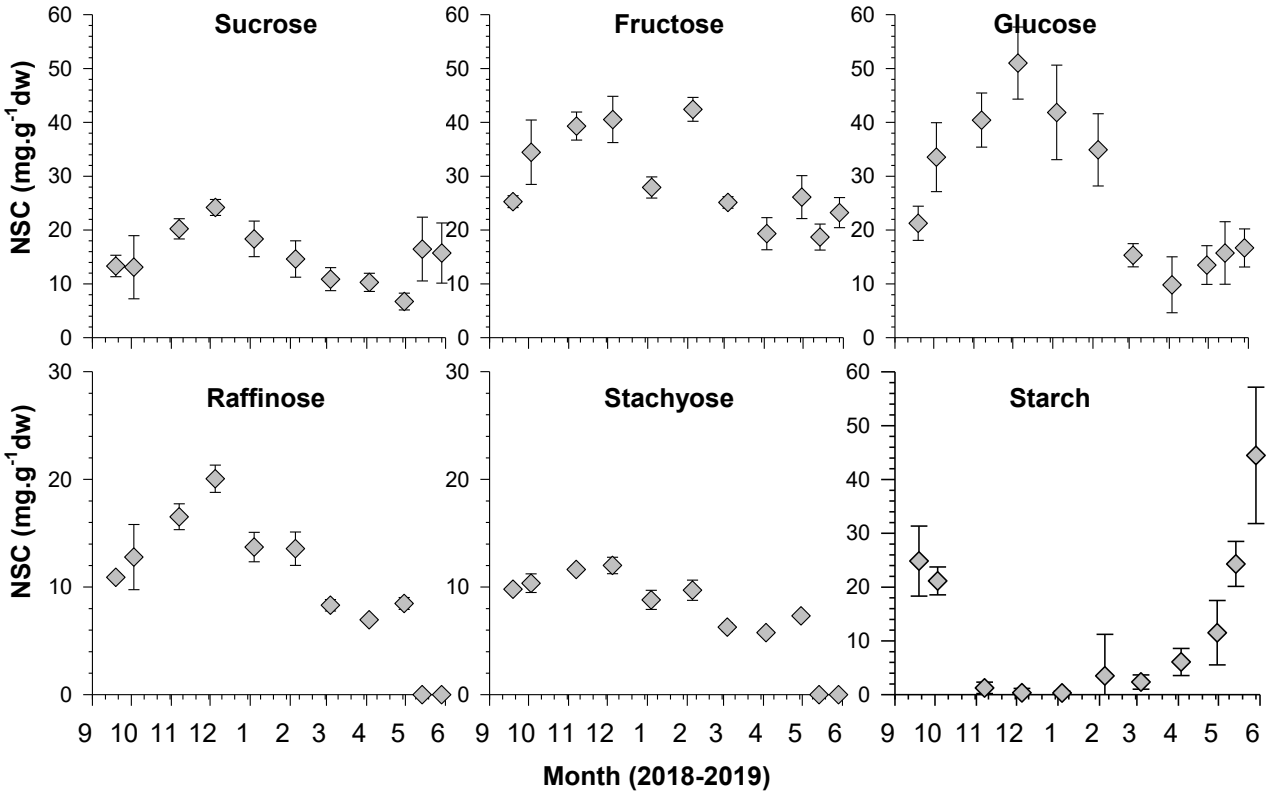

Figure 5. Variation in mean non-structural carbohydrates concentration (sucrose, glucose, fructose, raffinose, stachyose and starch), expressed in mg.g^{-1}dw in blueberry shoots. Note that the scales for

raffinose and stachyose differ from those for glucose, fructose, sucrose and starch. Vertical bars represent the standard deviation of the mean.

The PCA analysis described the relationships between variables representing the non-structural carbohydrates, LT_{50} and environmental cues (Figure 6). The first axis (PC1), explaining 54.1% of the total variance, divides samples from low (spring and early-autumn, on the right side) to high frost resistance (winter, on the left side) according to the variables that contribute the most to PC1 (LT_{50}, maximum temperature and photoperiod, Table 1). PC1 also defined two distinct groups of NSC: the soluble carbohydrates, negatively correlated with PC1 from starch, positively correlated with PC1 (Table 1).

Table 1. Correlation coefficients between the principal component axes PC1 and PC2 and the different variables used in the PCA with their contribution to axis definition (%).

		Variable	Correlation	P value	Contribution
PCA1	**Frost hardiness index**	LT_{50}	0.86	<0.001	11.47
	Environmental factors	Photoperiod	0.91	<0.001	12.87
		Tmin	0.73	<0.001	8.28
		Tmax	0.84	<0.001	10.89
		Tmean	0.80	<0.001	9.90
		Snow	-0.57	<0.001	5.02
	NSCs	Starch	0.78	<0.001	9.28
		Sucrose	-0.46	<0.001	3.25
		Glucose	-0.70	<0.001	7.51
		Fructose	-0.66	<0.001	6.77
		Stachyose	-0.63	<0.001	6.15
		Raffinose	-0.75	<0.001	8.61
PCA2	**Frost hardiness index**	LT_{50}	-0.04	0.700	0.05
	Environmental factors	Photoperiod	0.01	0.800	0.01
		Tmin	0.64	<0.001	13.09
		Tmax	0.49	<0.001	7.74
		Tmean	0.58	<0.001	10.59
		Snow	-0.73	<0.001	17.09
	NSCs	Starch	0.1	0.400	0.30
		Sucrose	0.51	<0.001	8.30
		Glucose	0.59	<0.001	10.86
		Fructose	0.53	<0.001	8.87
		Stachyose	0.62	<0.001	12.27
		Raffinose	0.58	<0.001	10.83

329 The second axis (PC2) explaining 26% of the total variance, mostly divides the samples belonging to the
330 acclimation period (first part of the hysteresis loop from September until December, on the top) from the
331 samples belonging to the deacclimation period (second part of the loop from January until June, on the
332 bottom) (Figure 6). Snow, mean and minimum temperature, stachyose, raffinose and glucose were the
333 main variables contributing to PC2 (Table 1). The soluble carbohydrates and temperature positively
334 correlated with the PC2 and corresponded to the samples belonging to the acclimation period. On the
335 contrary, snow depth was negatively correlated with PC2 (Table 1) and corresponded to samples
336 belonging to the winter months (mainly from January until March) when the snow was deeper (Figure 2).

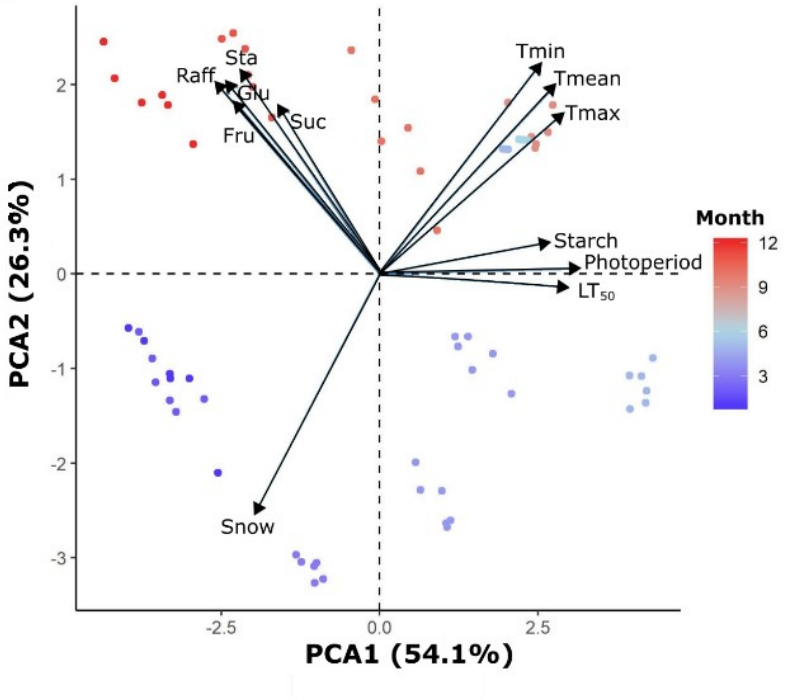

337 **Figure 6.** Principal component analysis (PCA) projecting different variables related with NSCs,
338 environmental cues and LT_{50}, according to different sampling times (months, represented by dots in
339 different colors). Only the first two axes are represented with the relative contribution explained. Suc,
340 sucrose; Fru, fructose; Glu, glucose; Raff, raffinose; Sta, stachyose.

3.4 Direct and indirect influence of environmental factors and non-structural carbohydrates on LT_{50}

Based on the hysteresis pattern and PCA analysis, we divided the dataset into two groups to test the influence of environmental factors and NSCs on LT_{50} (Figure 1): (1) cold acclimation, considering the sampling points from September 19th 2018 to January 4th 2019; (2) deacclimation, representing the period from January 4th to May 29th 2020. Because raffinose had the highest correlation with PC1, this carbohydrate was considered as representing the soluble carbohydrates dynamics in the SEM. Starch was also selected as it significantly contributed to PC1. Mean temperature was assumed to better reflect biological processes compared to minimum and maximum temperatures.

The SEMs suitably fitted our hypothesis (P_{bs}>0.05, CFI ≥0.95, SRMR<0.8), underlining the change in direct and indirect relationships between LT_{50}, NSCs and environmental factors between acclimation and deacclimation periods (Figure 7, Table 2). All SEMs were similar except for the environmental variable, the relative weight of which led to changes in coefficient values of the unchanged relationships between one model and the other. Indeed, environmental factors differed in the way they affect starch and raffinose concentrations, resulting in a different setup in their direct and indirect relationships. Among the environmental factors, snow cover showed the weakest sets of goodness of fit indexes (p=0.06, CFI=0.95, SMRS=0.03) (Figure 7).

During acclimation, photoperiod, mean temperature and raffinose were highly related to LT_{50} with R^2 that varied between 0.433 and 0.868 (Figure 7). During this stage, photoperiod was the most important explanatory variable, directly and positively related to LT_{50} (std=0.583), meaning that LT_{50} decreased at lower photoperiod. During acclimation, starch concentration depended on photoperiod (std=0.923) but the variation of photoperiod and variation of starch in relation to photoperiod did not directly influence the raffinose concentration (Table 2). Mean temperature also positively influenced LT_{50} (std=0.493), while snow cover had the lowest effect on cold hardiness, and was negatively related to Lt_{50} (std=-0.294). In all

364 models, LT_{50} decreased with increasing raffinose concentration. The raffinose concentration also
365 depended on snow cover (std=-0.36), indicating that the concentration of this carbohydrate increased with
366 a thinner snow cover. No direct effect of mean temperature was detected on raffinose, whose variability
367 was explained by the variation in starch (std=-0.991, R^2=0.497). Starch was affected by both mean
368 temperature and snow cover, and negatively influenced the raffinose concentration, i.e. higher
369 concentration was measured at lower starch level. All environmental variables strongly influenced starch
370 concentrations during acclimation: a lower starch concentration was related with a lower photoperiod
371 (std=0.932, R^2=0.868) and temperature (std=0.804, R^2=0.646), but at deeper snow level (-0.639,
372 R^2=0.408).

373 During the period of deacclimation (Figure 7, Table 2), the direct effects of photoperiod (std=0.304,
374 R^2=0.857) and temperature (std=0.330, R^2=0.859) were lower compared with the period of acclimation
375 (Figure 7) and no direct effect of snow cover on LT_{50} was detected at this stage (Table 2). Compared to
376 environmental factors, raffinose more fully explained LT_{50} during this period with coefficients ranging
377 from -0.652 to -0.865. Raffinose was directly and negatively linked to photoperiod and mean temperature
378 (std=-0.538 and -0.576, respectively), and starch (std=-0.477, R^2=0.768). As during acclimation, starch
379 was positively and directly related to photoperiod (std=0.734, R^2=0.538). Starch was also linked to all
380 environmental variables in a similar way to that of acclimation with R^2 varying between 0.5 to 0.9 (Figure
381 7).

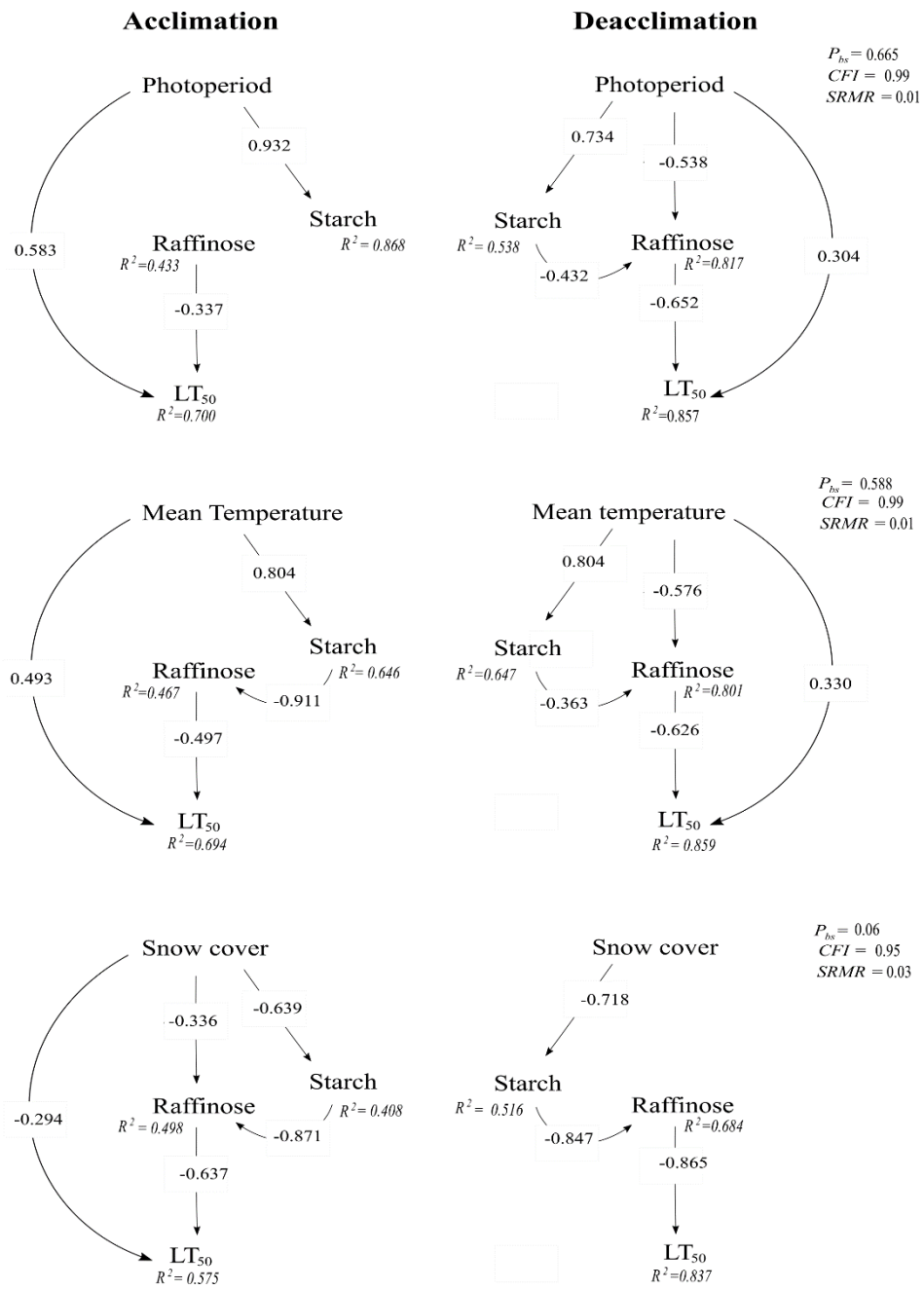

Figure 7. Structural equation model linking environmental [photoperiod, mean temperature (°C) and snow cover (cm), non-structural soluble carbohydrates (raffinose and starch, in mg. g^{-1}dw) and LT_{50} (°C). Only significant standardized coefficients are illustrated. Acclimation includes samples from September 2019 until January 2020 while deacclimation includes samples from January until May 2020. Bollen-Stine P-values (Pbs) and goodness of fit indexes (CFI and RSMR) are provided for each model.

Table 2. Standardized coefficients (STD coefficient), STD error, z-value and P value for all SEMs regressions.

Combination of variables		Regression	Variable	STD coefficient	STD error	z-value	P value
Photoperiod	Acclimation	LT_{50}	Raffinose	-0.337	0.512	-2.975	<0.05
			Photoperiod	0.583	0.021	3.941	<0.001
		Raffinose	Starch	-0.564	0.087	-1.701	0.089
			Photoperiod	-0.100	0.011	-0.271	0.787
		Starch	Photoperiod	0.932	0.09	12.714	<0.001
	Deacclimation	LT_{50}	Raffinose	-0.652	0.343	-5.039	<0.001
			Photoperiod	0.304	0.011	2.786	<0.05
		Raffinose	Starch	-0.432	0.04	-3.991	<0.001
			Photoperiod	-0.538	0.004	-5.335	<0.001
		Starch	Photoperiod	0.734	0.011	113.558	<0.001
Mean temperature	Acclimation	LT_{50}	Mean temperature	0.493	0.185	3.432	<0.01
			Raffinose	-0.497	0.468	-4.793	<0.001
		Raffinose	Starch	-0.911	0.058	-4.168	<0.001
			Mean temperature	0.317	0.066	1.368	0.171
		Starch	Mean temperature	0.804	0.101	8.592	<0.001
	Deacclimation	LT_{50}	Mean temperature	0.330	0.176	3.255	<0.001
			Raffinose	-0.626	0.35	-4.847	<0.001
		Raffinose	Starch	-0.363	0.044	-3.085	<0.001
			Mean temperature	-0.576	0.076	-5.100	<0.001
		Starch	Mean temperature	0.804	0.187	7.187	<0.001
Snow cover	Acclimation	LT_{50}	Raffinose	-0.637	0.529	-5.435	<0.001
			Starch	-0.294	0.122	-2.132	<0.05
		Raffinose	Starch	-0.871	0.036	-6.306	<0.001
			Snow	-0.336	0.029	-2.298	<0.05
		Starch	Snow	-0.639	0.082	-5.824	<0.001
	Deacclimation	LT_{50}	Raffinose	-0.865	0.284	-8.594	<0.001
			Snow	-0.082	0.036	-1.137	0.255
		Raffinose	Starch	-0.847	0.063	-4.907	<0.001
			Snow	-0.028	0.03	-0.158	0.874
		Starch	Snow	-0.718	0.067	-5.205	<0.001

4. Discussion

In wild blueberry, frost hardiness showed a transient increase and decrease from autumn to spring in response to both environmental factors and soluble carbohydrates – either directly or indirectly – in agreement with our hypothetical SEM. Our results highlighted two distinct periods of acclimation and deacclimation when environmental and biological regulation differed. Environmental factors were more closely linked to frost hardiness during cold acclimation [corresponding to the period between September and January (Charrier et al., 2011)] with a direct and indirect effect through starch degradation. This was also observed in highbush blueberry buds through protein profiling (Die et al., 2016). Autumn was characterized by the direct effect of environmental factors on starch hydrolysis increasing soluble carbohydrate contents. Later on, biological regulation, measured through soluble carbohydrates and especially raffinose, further induced a stronger direct regulation during the period of cold deacclimation, from January until the end of May at our sampling sites. Among the environmental factors, snow depth was the weakest correlated to frost hardiness, having no direct effect on raffinose concentrations during deacclimation.

4.1 Annual pattern of frost hardiness and REL curves

Woody plants from boreal regions are generally highly resistant to freezing temperature and can resist a wide range of low temperature (Strimbeck et al., 2015). Short days (e.g., photoperiods) alone has been shown sufficient to induce an initial stage of frost tolerance (Arora and Taulavuori, 2016; Schwarz, 1970). Accordingly, the frost hardiness (assessed by measuring LT_{50}) of blueberry stems already showed values <-20 °C in September. In September 2018, however, a single freeze-thaw event (minimum temperature of -0.5 °C) occurred 9 days before the first sampling date. From September 19th to October 3rd, REL curves shape changed drastically, indicating a rapid cold acclimation of the plants, early in autumn. Boreal species

413 acclimate rapidly, with the LN_2-quench tolerance (i.e. surviving liquid nitrogen immersion) already
414 acquired by late November (Strimbeck et al., 2008).

415 Maximum frost hardiness was reached between November and January, between -56 °C and -67 °.
416 Although litterature reported different acclimation timing during autumn, various highbush blueberry
417 genotypes reach maximum cold tolerance in mid-December (Rowland et al., 2008). In December, our
418 REL curves differed, exhibiting higher minimum REL, which could be related with native damage at the
419 moment of sampling, even if the samples from December were treated like those from other months.
420 Furthermore, 3 non-linear fits out of 6 samples were not significant in December while all other sampling
421 dates had significant fitting indicating that measurements could be affected by other factors during this
422 month. From our measurements, boreal blueberries (i.e. *V. angustifolium* and *V. myrtilloides*) can thus be
423 considered as extreme low temperature tolerant plants [ELT, <-60 °C, Strimbeck et al. (2015)]. At our
424 study site, the average minimum temperature in January is -22 °C with an absolute minimum that can
425 reach -40 °C (Environment Canada, 2019).Our observations on blueberry shoots combines both bark and
426 wood tissues, which are the most resistant organs, as observed in walnut trees (Charrier et al., 2013).

427 From April to end of May, the measured frost hardiness steadily increased from -40 to almost 0 °C.
428 *Vaccinium* spp. growing in the Alpine tundra in Switzerland exhibited similar frost hardiness: between -
429 25 °C (*Vaccinium vitis-idea* L.) and -15 °C (*V. myrtillus*) at the beginning of May (Palacio et al., 2015).
430 However, we observed that frost hardiness increased and decreased within the 15-day interval from mid-
431 May to mid-June, with the lowest frost hardiness (LT_{50} of -3.54 °C) measured at the end of snow melt.
432 Although only observed once in May, these variations could indicate a reacclimation pattern to cope with
433 highly variable temperature during springtime (Arora and Rowland, 2011; Arora and Taulavuori, 2016).
434 Rapid deacclimation in boreal areas can therefore represent an advantage to fully exploit the short
435 favorable growing season. In our site, during the months of May-June, temperatures above 20 °C are

436 frequent, but plants can still be exposed to freezing temperatures (see probability of freezing event in May
437 and June in the Walter & Lieth climatic diagrams, Figure 2). Sufficient and efficient reacclimation abilities
438 are thus highly desirable traits during springtime for plant survival in a highly variable environment (Arora
439 and Rowland, 2011).

440 ***4.2 Environmental cues driving the annual pattern of frost hardiness***

441 The process of cold acclimation and deacclimation generated clock-wise hysteretic loops that were closely
442 linked to environmental cues such as photoperiod and temperature. The influence of photoperiod
443 represented a consistent and astronomically controlled signal that is important in anticipated response by
444 regulating, via photoreceptors, the circadian clock (Ibáñez et al., 2010; Schultz and Kay, 2003). Exposure
445 to short day induces the acclimation of perennial shrubs and trees to cold temperature conditions by
446 altering the transcription of light signaling- and circadian clock-regulated genes (Maurya et al., 2018). In
447 *Rhododendron* plants, light signal (i.e. decreasing photoperiod) before low temperature was important to
448 further increase freezing tolerance (Liu et al., 2020), in agreement with our SEM results where photoperiod
449 was the most correlated factor during acclimation, followed by mean temperature. Snow depth was only
450 indirectly linked to frost hardiness through NSCs. Photoperiod was an important component of PC1 axes
451 such as frost hardiness (LT_{50}). As freezing is not an absolute requirement to reach low temperature
452 tolerance in early autumn (Strimbeck et al., 2008), photoperiod is probably a predominant factor in wild
453 blueberry in this period, followed by temperature (Li et al., 2004). Moreover, compared to temperature,
454 the hysteretic loop related to photoperiod was narrower. Such a differential behavior could lie in the
455 circadian clock regulation mediating the temperature-dependent processes of cold hardiness during
456 dormancy, as observed in hybrid poplar (Ibáñez et al., 2010).

457 Both our PCA and SEM results show that air temperature represents an important factor, especially during
458 acclimation. In trees derived from a high-elevation population of evergreen conifer *Abies sachalinensis*

459 Schmidt, frost hardiness develops earlier during acclimation compared to the low-elevation derived trees
460 (Ishizuka et al., 2015), demonstrating stronger temperature regulation when they are colder (Liu et al.,
461 2019). Also in walnut (*Junglans regia* L.), colder temperature accelerates the rate of frost hardening along
462 an altitudinal gradient (Charrier et al., 2011). Earlier frost hardiness in colder sites represents an ecological
463 adaptation by which plants reduce the length of the growing season, hence reducing the risk of frost
464 damage (Ishizuka et al., 2015), mostly caused by the minimum temperature of freezing events (Charrier
465 et al., 2018a). As frost events are highly probable in early September in boreal blueberry field, hardening
466 must be reached very early in fall. Our SEM results show that the decreasing temperature during autumn
467 also indirectly enables acclimation processes by influencing starch conversion to sugars, promoting the
468 synthesis of cryoprotectants. At similar daily temperature, frost hardiness was much lower during
469 acclimation than during deacclimation, generating a large hysteretic loop. In species such as *V. myrtillus*
470 growing in northern Finland, deacclimation follows temperature and therefore already exhibits
471 deacclimation in January (Taulavuori et al., 2002). A small rise in temperature, by 2-3 °C during winter
472 accelerates dehardening in *V. myrtillus*, with a reduced frost hardiness in heated plants (Taulavuori et al.,
473 1997). At our site, minimum temperatures were reached at the end of January, when LT_{50} values has
474 already started to increase. During deacclimation however, SEM showed that temperature has relatively
475 minor effects, as most of the variability in frost hardiness was explained by soluble carbohydrates such as
476 raffinose. From January to May, the regulation of frost hardiness could rely more on the internal
477 concentration of soluble carbohydrates (see next section) or other metabolites such as increased
478 antioxidants, proteins and amino acids (Bertrand et al., 2020; Die et al., 2016; Guy, 1990; Xin and Browse,
479 2000), thus exhibiting inertial response (Charrier et al., 2018b).

480 The snow depth is thinner in November – December compared to the January – March period: snow
481 started to accumulate only at mid-November and reached its peak level (about 80 cm) at the beginning of

March. SEM showed that snow depth was the least explanatory among the environmental factors, especially during the period of deacclimation when no direct effect of snow depth was observed on frost hardiness. During acclimation however, snow depth slightly affected frost hardiness (through positive correlation) and this variation was mainly driven by raffinose concentration (see next section). The deeper snow cover could offer a buffer to the variations in temperature, and especially the very low temperatures occurring in January – February, when most winter damage occurs (Girona et al., 2019). In our study, the temperature beneath the snow varied between two sampling points but was above -5 °C in February (see Figure 2, inset). However, the effect of snow depth on frost hardiness was not significant in eight Ericaceae species (Palacio et al., 2015), which could explain the absence of direct effect during deacclimation. Snow removal did not cause significant short-term damage in *V. myrtillus* (Tahkokorpi et al., 2007) although the absence of snow cover in the long term caused a significant loss of this understory plants (Kreyling et al., 2012). Underground parts usually remain relatively protected by the insulating effect of snow and the thermal inertia of the soil, a decrease in snow depth can thus impair not only the aboveground parts but also roots (Ambroise et al., 2020), leading to decreased plant productivity and survival. Moreover, snow also offers protection against winter desiccation (Taulavuori et al., 2011).

However, measuring snow depth directly at sampling sites could have led to better correlation coefficients in SEM, as snow depth may strongly vary locally, within the same field (Girona et al., 2019). Another way to improve our models would have been to use the monitoring of air temperature underneath the snow cover, directly at the wild blueberry plant level, but our system failed to work until February. Such monitoring has the advantage of taking into consideration air temperatures and snow depth at the same time (at the same measurement), but it also has the disadvantage of reducing the applicability potential of our models, as temperature sensors are not routinely positioned beneath the snow cover for most publicly-available weather stations.

505 ***4.3 Effect of non-structural carbohydrate on frost hardiness***

506 Cold acclimation is often associated with changes in carbohydrates metabolism including a decrease in
507 starch and an increase in soluble carbohydrates, such as raffinose (Beauvieux et al., 2018; Charrier et al.,
508 2013; Kasuga et al., 2007). Starch reserves in the blueberry shoot were rapidly degraded, already reaching
509 zero at the beginning of November. Transcripts of a protein modulating the activity of starch degrading
510 enzymes (DSP4) in the phloem parenchyma cells remain high from autumn to spring, with highest
511 expression during October (Berrocal-Lobo et al., 2011). In highbush blueberry (*Vaccinium corymbosum*
512 L.), starch content also decreases in the middle of cold acclimation and coincides with β-amylase gene
513 expression (Lee et al., 2012). The α-amylase, β-amylase and starch phosphorylase activities exhibit a
514 positive correlation with the decrease in temperature (Kasuga et al., 2007), explaining the positive
515 influence of temperature on starch content in SEM. Shorter photoperiods during acclimation also influence
516 starch degradation as shown by the direct effect of photoperiod on starch content in the SEM and the
517 positive correlation of starch and photoperiod with PC1.

518 In all models (except for photoperiod during acclimation), a decrease in starch was correlated to an
519 increase in soluble carbohydrates, such as raffinose. Raffinose was then directly and negatively correlated
520 to frost hardiness. The hydrolysis of starch stored in amyloplasts helps in producing, from starch-maltose
521 conversion, oligosaccharides such as sucrose, raffinose and stachyose (Sauter, 1988). These soluble
522 compounds increased in blueberry stem during autumn as the air temperature gradually dropped. Snow
523 depth also negatively influenced raffinose content: during acclimation, beneath thinner snow, lower
524 minimum temperatures would be reached, hence increasing raffinose content. A decoupling effect in the
525 direct influence of photoperiod and starch raffinose concentration was observed during acclimation:
526 raffinose was indeed strongly correlated with both photoperiod and starch ($R_{Pearson}$=-0.7, $p<0.05$, data not

shown) but the direct link between starch and raffinose in the SEM model was not significant (std=-0.564, P=0.089).

In *V. corymbosum*, the soluble carbohydrates that were strongly associated with frost resistance were raffinose, glucose and fructose (Lee et al., 2012). In our study, stachyose was also detected with a concentration higher than 10 $mg.g^{-1}$dw during winter, as also observed in boreal conifers (Strimbeck et al., 2008). Our PCA analysis revealed that stachyose was highly correlated to raffinose. In contrast, monosaccharides, especially glucose, still increased during November and December. As proposed by Beauvieux et al. (2018), the gluconeogenesis pathway can produce glucose from storage lipids and amino acids. In our study, both glucose and fructose were the most abundant solutes during the maximum of frost hardiness in December. Energy metabolism is essential to survive during a long winter as shown by an increased level of proteins involved in glycolysis during cold acclimation (Die et al., 2016). Glucose has a fundamental role during dormancy being metabolized in at least three pathways for detoxification (by the pentose phosphate pathway), mitochondrial respiration (by glycolysis) and lactate production (by fermentation) (Beauvieux et al., 2018). Therefore, glucose and fructose contents are not great predictors of frost hardiness for our *Vaccinium* species.

During deacclimation, our results showed that a combination of raffinose and mean temperature or raffinose and photoperiod explained a large proportion of frost hardiness variability (86 and 88%, respectively). In all models, raffinose was directly linked to frost hardiness, as observed in several boreal conifer species (Strimbeck et al., 2008). However, higher temperature directly reduced the raffinose concentration, such as during a winter warming experiment on *V. myrtillus* (Bokhorst et al., 2010), increasing the vulnerability of wild blueberries to winter warming events. Raffinose maintains membrane integrity under abiotic stress as well as ROS scavenging. Furthermore, Raffinose Family Oligosaccharides (RFOs) facilitate vitrification and prevent sucrose from crystallizing (dos Santos et al., 2011; Nishizawa-

550 Yokoi et al., 2008). Preventing sucrose crystallizing during winter desiccation, after extracellular freezing,
551 preserves its cryoprotective effect, by maintaining the hydroxyl groups of sucrose to replace water in the
552 phospholipid groups of the membrane (ElSayed et al., 2014; Imanishi et al., 1998). In contrast to red
553 raspberry (Palonen et al., 2000), the disaccharide sucrose remained relatively low during winter compared
554 to monosaccharides. However, as raffinose and stachyose are formed by the addition of a galactinol unit
555 to sucrose (Castillo et al., 1990; Nishizawa-Yokoi et al., 2008), this could prevent sucrose concentration
556 increasing during winter, as during drought in boreal trees (Deslauriers et al., 2014).

557 **5. Conclusion**

558 Multiple environmental stimuli were either directly or indirectly linked, through NSCs, to the level of
559 frost hardening in wild blueberry *V. angustifolium* and *V. myrtiloides*. However, the importance of
560 environmental factors differed between cold acclimation and deacclimation, being more important during
561 acclimation when higher frost hardiness (i.e. lower LT_{50}) is reached. Frost hardiness rapidly decreases as
562 temperatures rise during spring making wild blueberry stems more vulnerable during deacclimation
563 compared to the acclimation period. During the period of cold deacclimation, direct biological regulation
564 through raffinose defined most of the frost hardiness but a negative influence of temperature on this
565 important carbohydrate could increase vulnerability to winter warming events. In commercial wild
566 blueberry fields, winter frost damage is a major threat and may reduce fruit yield by more than 50%, as
567 observed in our study area in 2015 (Girona et al., 2019). As winter frost damage generally occurs during
568 deacclimation period, our results suggest that raffinose contents could be potentially used as predictor of
569 winter frost damage (Figure 7). Indeed, combined with air temperature data, plant raffinose content may
570 represent a relatively easy, rapid, and quantitative way to indirectly estimate the probability of frost
571 damage during the plant deacclimation period, and hence help producers and agronomists to better plan,
572 at the field scale, management practices that should be performed in early spring (e.g., prescribing

573 pruning), when the buds are not yet open. Because commercial wild blueberry fields are managed over a
574 2-year crop cycle (i.e., pruning year followed by a fruit harvesting year), not mowing damaged fields in
575 early spring increases winter frost consequences over a longer period of time (>2 years).

576 **Acknowledgments**

577 The authors thank the Natural Sciences and Engineering Research Council of Canada (NSERC) (Grant
578 RDCPJ-503182-16), and the *Fonds de recherche axé sur l'agriculture nordique* for their financial support.
579 The authors also thank *Les Entreprises Gérard Doucet Ltée*, who provided access to their sites and
580 infrastructure.

581

References

Ambroise, V. et al., 2020. The roots of plant frost hardiness and tolerance. Plant Cell Physiol., 61(1): 3-20.

Anderson, C.I. and Gough, W.A., 2017. Evolution of winter temperature in Toronto, Ontario, Canada: A case study of winters 2013/14 and 2014/15. Journal of Climate, 30(14): 5361-5376.

Arora, R. and Rowland, L.J., 2011. Physiological research on winter-hardiness: Deacclimation resistance, reacclimation ability, photoprotection strategies, and a cold acclimation protocol design. Hortscience, 46(8): 1070-1078.

Arora, R. and Taulavuori, K., 2016. Increased risk of freeze damage in woody perennials VIS-À-VIS climate change: Importance of deacclimation and dormancy response. Frontiers in Environmental Science, 4: 44.

Baffoin, R., Charrier, G., Bouchardon, A.E., Bonhomme, M. and Lacointe, A., 2020. Differential effect of carbohydrates on osmotic control of tree frost tolerance in various temperate tree species. Tree Physiol., Submitted.

Beaujean, A.A., 2014. Latent variable modeling using R: A step-by-step guide. Routledge.

Beauvieux, R., Wenden, B. and Dirlewanger, E., 2018. Bud dormancy in perennial fruit tree species: A pivotal role for oxidative cues. Front. Plant Sci., 9: 657.

Bellasio, C., Fini, A. and Ferrini, F., 2014. Evaluation of a high throughput starch analysis optimised for wood. PLoS One, 9(2): e86645.

Berrocal-Lobo, M. et al., 2011. Identification of a homolog of Arabidopsis DSP4 (SEX4) in chestnut: Its induction and accumulation in stem amyloplasts during winter or in response to the cold. Plant, Cell and Environment, 34(10): 1693-1704.

Bertrand, A. et al., 2020. Biochemical and molecular responses during overwintering of red clover populations recurrently selected for improved freezing tolerance. Plant Sci., 292: 15.

Bokhorst, S. et al., 2010. Impacts of extreme winter warming events on plant physiology in a sub-Arctic heath community. Physiol. Plant., 140(2): 128-140.

Bonham, C.D., 2013. Measurements for Terrestrial Vegetation, Second Edition. John Wiley & Sons.

Cappiello, P.E. and Dunham, S.W., 1994. Seasonal variation in low-temperature tolerance of *Vaccinium angustifolium* Ait. Hortscience, 29(4): 302-304.

Castillo, E.M., De Lumen, B.O., Reyes, P.S. and De Lumen, H.Z., 1990. Raffinose synthase and galactinol synthase in developing seeds and leaves of legumes. J. Agric. Food Chem., 38(2): 351-355.

Charrier, G., Bonhomme, M., Lacointe, A. and Améglio, T., 2011. Are budburst dates, dormancy and cold acclimation in walnut trees (Juglans regia L.) under mainly genotypic or environmental control? International journal of biometeorology, 55(6): 763-774.

Charrier, G., Chuine, I., Bonhomme, M. and Améglio, T., 2018a. Assessing frost damages using dynamic models in walnut trees: exposure rather than vulnerability controls frost risks. Plant, Cell & Environment, 41(5): 1008-1021.

Charrier, G., Lacointe, A. and Améglio, T., 2018b. Dynamic modeling of carbon metabolism during the dormant period accurately predicts the changes in frost hardiness in walnut trees *Juglans regia* L. Front. Plant Sci., 9: 1746.

Charrier, G., Poirier, M., Bonhomme, M., Lacointe, A. and Ameglio, T., 2013. Frost hardiness in walnut trees (Juglans regia L.): How to link physiology and modelling? Tree Physiol., 33(11): 1229-1241.

Deslauriers, A. et al., 2014. Impact of warming and drought on carbon balance related to wood formation in black spruce. Ann. Bot., 114(2): 335-345.

Die, J.V., Arora, R. and Rowland, L.J., 2016. Global patterns of protein abundance during the development of cold hardiness in blueberry. Environ. Exp. Bot., 124: 11-21.

Die, J.V. and Rowland, L.J., 2014. Elucidating cold acclimation pathway in blueberry by transcriptome profiling. Environ. Exp. Bot., 106: 87-98.

dos Santos, T.B. et al., 2011. Expression of three galactinol synthase isoforms in Coffea arabica L. and accumulation of raffinose and stachyose in response to abiotic stresses. Plant Physiol. Biochem., 49(4): 441-448.

ElSayed, A., Rafudeen, M. and Golldack, D., 2014. Physiological aspects of raffinose family oligosaccharides in plants: protection against abiotic stress. Plant Biol., 16(1): 1-8.
Environment Canada, 2019. Historical climate data.
Fournier, M.-P. et al., 2020. How plant allometry influences bud phenology and fruit yield in two Vaccinium species. Ann. Bot., In press: mcaa083.
Girona, J., Bradley, R., Lévesque, J.-A., Paré, M. and Bellemare, M., 2019. A call For improving winter windbreak design for lowbush blueberry production in the Saguenay–Lac-Saint-Jean region of Québec, Canada. International Journal of Fruit Science, 19(2): 165-178.
Grace, J.B., 2006. Structural equation modeling and natural systems. Cambridge University Press, Cambridge UK.
Guy, C.L., 1990. Cold acclimation and freezing stress tolerance: role of protein metabolism. Annual Review of Plant Biology, 41(1): 187-223.
Hooper, D., Coughlan, J. and Mullen, M., 2008. Structural equation modelling: guidelines for determining model fit. Electron J Bus Res Methods 6: 53-60.
Ibáñez, C. et al., 2010. Circadian clock components regulate entry and affect exit of seasonal dormancy as well as winter hardiness in *Populus* trees. Plant Physiol., 153(4): 1823-1833.
Imanishi, H.T., Suzuki, T., Masuda, K. and Harada, T., 1998. Accumulation of raffinose and stachyose in shoot apices of Lonicera caerulea L. during cold acclimation. Sci. Hortic., 72(3-4): 255-263.
Ishizuka, W., Ono, K., Hara, T. and Goto, S., 2015. Use of intraspecific variation in thermal responses for estimating an elevational cline in the timing of cold hardening in a sub-boreal conifer. Plant Biol., 17(1): 177-185.
Kasuga, J., Arakawa, K. and Fujikawa, S., 2007. High accumulation of soluble sugars in deep supercooling Japanese white birch xylem parenchyma cells. New Phytol., 174(3): 569-579.
Kreyling, J., Haei, M. and Laudon, H., 2012. Absence of snow cover reduces understory plant cover and alters plant community composition in boreal forests. Oecologia, 168(2): 577-587.
Lee, J.H., Yu, D.J., Kim, S.J., Choi, D. and Lee, H.J., 2012. Intraspecies differences in cold hardiness, carbohydrate content and β-amylase gene expression of Vaccinium corymbosum during cold acclimation and deacclimation. Tree Physiol., 32(12): 1533-1540.
Lee, J.I., Yu, D.J., Lee, J.H., Kim, S.J. and Lee, H.J., 2013. Comparison of mid-winter cold-hardiness and soluble sugars contents in the shoots of 21 highbush blueberry (*Vaccinium corymbosum*) cultivars. J. Horticult. Sci. Biotechnol., 88(6): 727-734.
Li, C., Junttila, O. and Palva, E.T., 2004. Environmental regulation and physiological basis of freezing tolerance in woody plants. Acta Physiol. Plant., 26(2): 213-222.
Liu, B. et al., 2020. Factors affecting freezing tolerance: a comparative transcriptomics study between field and artificial cold acclimations in overwintering evergreens. The Plant Journal, 103(6): 2279-2300.
Liu, B., Xia, Y.-p., Krebs, S.L., Medeiros, J. and Arora, R., 2019. Seasonal responses to cold and light stresses by two elevational ecotypes of Rhododendron catawbiense: A comparative study of overwintering strategies. Environ. Exp. Bot., 163: 86-96.
MAPAQ, Ministère de l'Agriculture, des Pêcheries et de l'Alimentation du Québec., 2016. Monographie de l'industrie du bleuet sauvage au Québec. Gouvernement du Québec, pp. 32.
Maurya, J.P., Triozzi, P.M., Bhalerao, R.P. and Perales, M., 2018. Environmentally sensitive molecular switches drive Poplar phenology. Front. Plant Sci., 9: 1873.
Moore, J.N., 1994. The blueberry industry of North America. Hort Technology 3(4): 96-102.
Nishizawa-Yokoi, A., Yabuta, Y. and Shigeoka, S., 2008. The contribution of carbohydrates including raffinose family oligosaccharides and sugar alcohols to protection of plant cells from oxidative damage. Plant Signaling & Behavior, 3(11): 1016-1018.
Palacio, S., Lenz, A., Wipf, S., Hoch, G. and Rixen, C., 2015. Bud freezing resistance in alpine shrubs across snow depth gradients. Environmental and Experimental Botany, 118: 95-101.
Palonen, P., Buszard, D. and Donnelly, D., 2000. Changes in carbohydrates and freezing tolerance during cold acclimation of red raspberry cultivars grown in vitro and in vivo. Physiol. Plant., 110(3): 393-401.

Rosseel, Y., 2012. Lavaan: An R package for structural equation modeling and more. Version 0.5–12 (BETA). Journal of Statistical Software, 48(2): 1-36.
Rowland, L.J., Ogden, E.L., Ehlenfeldt, M.K. and Arora, R., 2008. Cold tolerance of blueberry genotypes throughout the dormant period from acclimation to deacclimation. Hortscience, 43(7): 1970-1974.
Saarinen, T. and Lundell, R., 2010. Overwintering of Vaccinium vitis-idaea in two sub-Arctic microhabitats: a reciprocal transplantation experiment. Polar Res., 29(1): 38-45.
Sauter, J.J., 1988. Temperature-induced changes in starch and sugars in the stem of *Populus* × *canadensis* «robusta». J. Plant Physiol., 132(5): 608-612.
Schultz, T.F. and Kay, S.A., 2003. Circadian clocks in daily and seasonal control of development. Science, 301(5631): 326-328.
Schwarz, W., 1970. Der einfluß der photoperiode auf das austreiben, die frosthärte und die hitzeresistenz von zirben und alpenrosen. Flora, 159(3): 258-285.
Strimbeck, G.R., Kjellsen, T.D., Schaberg, P.G. and Murakami, P.F., 2008. Dynamics of low-temperature acclimation in temperate and boreal conifer foliage in a mild winter climate. Tree Physiol., 28(9): 1365-1374.
Strimbeck, G.R., Schaberg, P.G., Fossdal, C.G., Schröder, W.P. and Kjellsen, T.D., 2015. Extreme low temperature tolerance in woody plants. Front. Plant Sci., 6: 884.
Tahkokorpi, M., Taulavuori, K., Laine, K. and Taulavuori, E., 2007. After-effects of drought-related winter stress in previous and current year stems of Vaccinium myrtillus L. Environ. Exp. Bot., 61(1): 85-93.
Taulavuori, K., Bauer, E. and Taulavuori, E., 2011. Overwintering stress of Vaccinium vitis-idaea in the absence of snow cover. Environ. Exp. Bot., 72(3): 397-403.
Taulavuori, K., Laine, K. and Taulavuori, E., 2002. Artificial deacclimation response of Vaccinium myrtillus in mid-winter, Annales Botanici Fennici. JSTOR, pp. 143-147.
Taulavuori, K., Laine, K., Taulavuori, E., Pakonen, T. and Saari, E., 1997. Accelerated dehardening in bilberry (Vaccinium myrtillus L.) induced by a small elevation in air temperature. Environ. Pollut., 98(1): 91-95.
Vander Kloet, S.P., 1988. The genus Vaccinium in North America. Agriculture Canada, Gouvernement du Canada, 218 pp.
Wildung, D.K. and Sargent, K., 1989. The effect of snow depth on winter survival and productivity of Minnesota blueberries. Acta Horticulturae(241): 232-237.
Williams, C.M., Henry, H.A. and Sinclair, B.J., 2015. Cold truths: how winter drives responses of terrestrial organisms to climate change. Biological Reviews, 90(1): 214-235.
Xin, Z. and Browse, J., 2000. Cold comfort farm: the acclimation of plants to freezing temperatures. Plant, Cell & Environment, 23(9): 893-902.
Yu, B. and Zhang, X., 2015. A physical analysis of the severe 2013/2014 cold winter in North America. Journal of Geophysical Research: Atmospheres, 120(19): 10,149-10,165.
Zhang, G., Ryyppo, A., Vapaavuori, E. and Repo, T., 2003. Quantification of additive response and stationarity of frost hardiness by photoperiod and temperature in Scots pine. Can. J. For. Res.-Rev. Can. Rech. For., 33(9): 1772-1784.
Zuur, A.F., Ieno, E.N. and Elphick, C.S., 2010. A protocol for data exploration to avoid common statistical problems. Methods in Ecology and Evolution, 1: 3-14.

Captions 'list

Figure 1. Assumptions behind the conceptualization of the structural equation models (SEM) linking environmental variables, NSCs and frost hardiness index. In the middle, the structure of raffinose (left) and glucose (right) represent examples of NSCs.

Figure 2. Left part: Maximum (black line) and minimum (gray line) air temperature (°C) and snow depth (gray background, cm) recorded at the Bagotville station from September 2018 to July 2019. Inset: Mean temperature (°C) at the soil-snow interface, at two sampling points from February to May 2020. Right part: Walter & Lieth climatic diagrams representing average climatic conditions [mean temperature (red line), mean precipitation (in blue)] at the nearest weather station (Bagotville). The blue rectangles represent months with below zero temperature while the cyan rectangles indicate months when below zero temperatures are highly probable.

Figure 3. Left part: Relationships between electrolyte leakage (REL) and temperature (°C) calculated according to a sigmoidal relationship for the different sampling dates by using all transect sampling points. Curve fittings were performed by using all transect data points (black dots, illustrated in the graph on the left). Right part: LT_{50} (°C) of each transect line (black dots) and mean LT_{50} (gray square) for the different sampling dates.

Figure 4. Higher part: Seasonal hysteresis between LT_{50} (°C) and meteorological variables [maximum, mean, and minimum temperature (°C) averaged over 5 days, snow depth (cm), and photoperiod (hour)] at monthly scale. Lower part: Relationship between LT_{50} (°C) and soluble sugars [sucrose, glucose, fructose, stachyose and raffinose, expressed in $mg.g^{-1}dw$]. Seasonal hysteresis between LT_{50} (°C) and starch concentration ($mg.g^{-1}dw$). The direction of the hysteresis, if present, is indicated with an arrow.

Figure 5. Variation in mean non-structural carbohydrates concentration (sucrose, glucose, fructose, raffinose, stachyose and starch), expressed in $mg.g^{-1}dw$ in blueberry shoots. Note that the scales for

raffinose and stachyose differ from those for glucose, fructose, sucrose and starch. Vertical bars represent the standard deviation of the mean.

Figure 6. Principal component analysis (PCA) projecting different variables related with NSCs, environmental cues and LT_{50}, according to different sampling times (months, represented by dots in different colors). Only the first two axes are represented with the relative contribution explained. Suc, sucrose; Fru, fructose; Glu, glucose; Raff, raffinose; Sta, stachyose.

Figure 7. Structural equation model linking environmental [photoperiod, mean temperature (°C) and snow cover (cm), non-structural soluble carbohydrates (raffinose and starch, in mg. g^{-1}dw) and LT_{50} (°C). Only significant standardized coefficients are illustrated. Acclimation includes samples from September 2019 until January 2020 while deacclimation includes samples from January until May 2020. Bollen-Stine P-values (Pbs) and goodness of fit indexes (CFI and RSMR) are provided for each model.

Table 1. Correlation coefficients between the principal component axes PC1 and PC2 and the different variables used in the PCA with their contribution to axis definition (%).

Table 2. Standardized coefficients (STD coefficient), STD error, z-value and P value for all SEMs regressions.

Supplementary Figures

Figure S1. Sampling at one transect point in February. The blueberry stems were dig up by removing the snow in a surface of about 2 meters long × 1 meter large. The higher portion of one stem was cut due to ice formation at the soil surface. It was not possible to distinguish the stems belonging to the species *Vaccinium angustifolium* or *Vaccinium myrtilloides* under the snow during winter. Therefore, both species were simultaneously sampled.

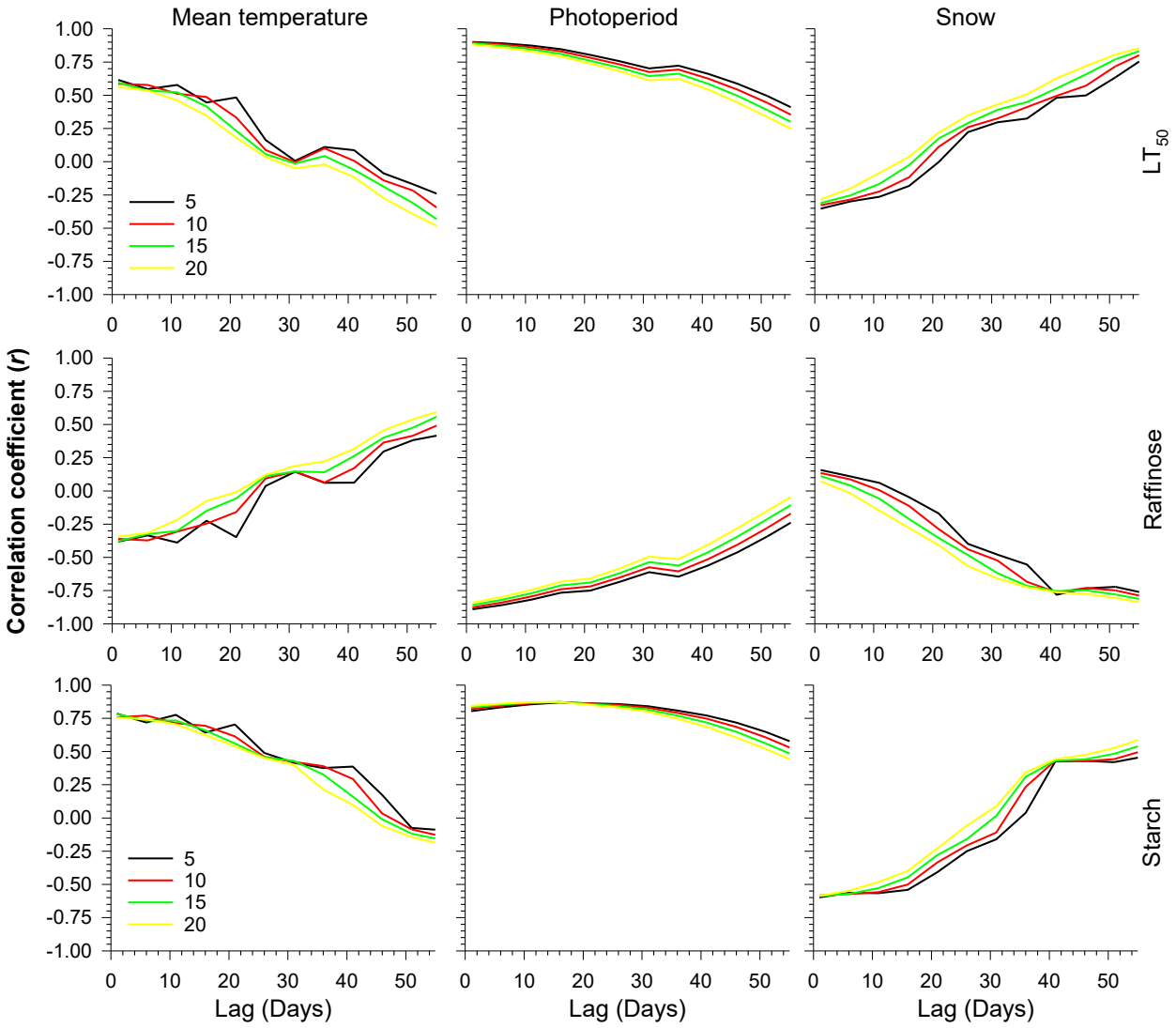

Figure S2. Variation of the correlation coefficient (*r*, Pearson) between LT_{50}, raffinose and starch and environmental variables (mean temperature, photoperiod and snow level). We use different time windows (between 5 and 20 days) to calculate means environmental parameters and different time lag (from 1 to 55 days) before the sampling. For example, for a window of 5 day, we calculate mean environmental parameter by including the 1^{rst} to the 6^{th} day prior to the sampling at lag 1, then the second to the 7 at lag 2. Then, the different combination of time window and lag were correlated either with LT_{50} or NSC values.